



The Solubility of Deep Eutectic Solvents Derived from Allyltriphenylphosphonium Bromide in Supercritical Carbon Dioxide in the Presence of Ethanol as a Cosolvent

YoonKook Park¹

Received: 5 December 2023 / Revised: 8 January 2024 / Accepted: 12 January 2024 / Published online: 15 February 2024
© The Author(s), under exclusive licence to Korean Institute of Chemical Engineers, Seoul, Korea 2024

Abstract

Two distinct deep eutectic solvents (DESs) were prepared by combining allyltriphenylphosphonium bromide (ATPPB) as a hydrogen bond acceptor (HBA) and ethylene glycol as a hydrogen bond donor (HBD) at molar ratios of 6:1 and 8:1, respectively. The study investigated the solubility of these DESs in supercritical carbon dioxide, with ethanol serving as a cosolvent, under varying conditions of temperatures 308.2, 313.2, and 318.2 K and pressures up to 18.89 MPa. Solubilities were determined by measuring both bubble point and cloud point pressures in ternary mixtures comprising CO₂, ethanol, and DES, utilizing a phase equilibrium apparatus equipped with a high-pressure variable-volume view cell. Higher molar ratios between ethylene glycol and ATPPB resulted in significantly higher pressures required for the solubility of DES. The occurrence of either bubble point or cloud point depended on the molar ratios between the cosolvent (ethanol) and the solvent (scCO₂) for both DESs. Increasing system temperature at a constant DES mole fraction led to an elevation in both bubble point and cloud point pressures. Furthermore, an increases in the amount of cosolvent (ethanol) resulted in a substantial decrease in both bubble point and cloud point pressures. The experimental data exhibited robust correlation with three models: the modified Chrastil equation, the Kumar–Johnston equation, and the Adachi–Lu equation.

Keywords Deep eutectic solvent · Supercritical fluids · Cosolvent

Introduction

Supercritical carbon dioxide (scCO₂), deep eutectic solvents (DESs), and ionic liquids have gained significant attention in recent years due to their unique properties and versatile applications in various fields. scCO₂ refers to CO₂ at a temperature and pressure above its critical point. In this state, CO₂ exhibits both gas and liquid-like properties, making it an environmentally friendly solvent for a wide range of substances. Researchers have been exploring the solubility of different compounds in scCO₂ to develop environmentally friendly process. Unfortunately, although it can solubilize low molecular weight, volatile compounds, polar and high-molecular weight materials, CO₂ is a feeble solvent, as Beckman reported [1]. Great progress has been made in

disclosing hydrocarbon-based CO₂-philic containing carbonyl groups, which are known to interact through a Lewis acid–Lewis base interaction with CO₂ molecules [2–4]. In addition, phosphorus compounds, particularly phosphonium-based salts, are known to enhance CO₂ solubility [5, 6].

DESs are often composed of inexpensive and readily available components of a hydrogen bond donor (HBD) and a hydrogen bond acceptor (HBA). This makes them more cost-effective compared to many ionic liquids, which often involve more complex and costly synthesis processes [7]. DESs, in many cases, exhibit higher biodegradability compared to ionic liquids. The use of natural or bio-derived components in DES contributes to their more environmentally friendly profile. In particular, the selection of allylphosphonium salts for preparing DESs is driven by their versatile and tunable properties, polar nature, and compatibility with green chemistry principles [8–10]. Dialcohols, such as, ethylene glycol, are favored for preparing DES due to hydrogen bond donor capability, tunable properties, biodegradability, and low toxicity [11–13].

✉ YoonKook Park
parky@hongik.ac.kr

¹ Department of Bio. and Chemical Engineering, Hongik University, Sejong 30016, South Korea

As far as extension of scCO_2 usage is concerned higher solubility of versatile chemicals can also be easily accomplished in the presence of polar cosolvent with hydrogen bond capacity. Brennecke et al. [14]. investigated the phase behavior of systems combining scCO_2 with ionic liquids. The findings revealed unexpectedly high solubility of CO_2 in five ionic liquids, while the solubility of ionic liquids in scCO_2 was notably low, approximately on the order of 10^{-7} . Numerous studies [15–18] have explored the impact of cosolvents on the solubility of ionic liquids in scCO_2 . These investigations revealed that the solubility of ionic liquids in scCO_2 was remarkably low. However, the addition of cosolvent proved to be a significant factor in substantially augmenting the solubility of ionic liquids in scCO_2 . Although the solubility of DES in scCO_2 surpasses that of ionic liquid in scCO_2 [18–20], there remains considerable potential for improvement in the presence of a cosolvent.

Emerging computational methodologies, such as artificial intelligences [21] and group theory [22] offer the capability to predict solubility data with exceptional accuracy. However, the effective training of these models necessitates extensive and precise experimental information, which is often scarce across various temperature and pressure ranges. Consequently, empirical and semi-empirical models have proven successful in correlating solubility data with high efficacy [23–26]. These models, particularly empirical ones, offer simplicity in application, where the solubility of a substance is influenced by density, pressure, and temperature of scCO_2 in the presence of a cosolvent.

The mole ratios between HBD and HBA play a crucial role in determining the formation of DES and influencing the appropriate viscosity range [19]. In this study, two DESs were formulated employing ethylene glycol as the HBD and allytriphenylphosphonium bromide as the HBA, with mole ratios specified as 6 to 1 (E6A1) and 8 to 1 (E8A1), respectively. Typically, extractions are conducted at pressures of 7–14 MPa and temperatures of 308–343 K [27]. To assess the solubility of these DESs, evaluations were carried out in scCO_2 as the solvent, along with ethanol as a cosolvent. The evaluations encompassed a temperature range of 308.2 to 318.2 K at intervals of 5 K to explore temperature effects. Furthermore, the study delved into the impact of system density and mole ratio between the solvent and cosolvent on DES solubility. Experimental results were then correlated using distinct empirical models: the modified Chrastil equation [24], the Kumar–Johnston equation [25], and the Adachi–Lu equation [26].

Table 1 List of chemical used in this study

Compound	CAS-No	Supplier	Purity (%)
Allyltriphenylphosphonium bromide (ATPPB)	1560–54-9	Merck Inc	99
Ethylene glycol (EG)	107-21-1	Merck Inc	≥ 99
Ethanol	64-17-5	Merck Inc	≥ 99.5
Carbon dioxide (CO_2)	124-38-9	Sebotech Inc	≥ 99.9

Table 2 The molecular weights of the compounds employed and prepared in this study

Compound	$\text{M/g}\cdot\text{mol}^{-1}$
Ethylene glycol (EG)	62.07
Allyltriphenylphosphonium bromide (ATPPB)	383.26
E6A1	107.96
E8A1	97.76

Experimental

Chemicals and preparation of the DESs

Ethylene glycol, ethanol, and allyltriphenylphosphonium bromide (ATPPB) were purchased from Merck Inc, as shown in Table 1. The supercritical fluid chromatography grade carbon dioxide was sourced from Sebotech Inc. (Sejong, Korea). All chemicals were utilized as received without further purification. Two DESs, denoted as E6A1 and E8A1, were formulated using ethylene glycol and ATPPB with mole ratios of 6:1 and 8:1, respectively. The molecular weight of the prepared DES was calculated based on the individual compounds, as per Eq. (1).

$$M_{DES} = x_{EG}M_{EG} + x_{ATPPB}M_{ATPPB} \quad (1)$$

where M_i and x_i refer to the molecular weight and mole fraction of compound i . Molecular weights ($\text{g}\cdot\text{mol}^{-1}$) of E6A1 and E8A1 DESs are 107.95 and 97.96, respectively, as shown in Table 2. The water content in the prepared DESs was determined using a Karl-Fisher titrator (Model V20). The analysis indicated that the water content for E6A1 and E8A1 is 0.07% and 0.09%, respectively.

Experimental Apparatus and Method

The experimental apparatus and methodology employed to ascertain the phase behavior have been previously elucidated [28–30]. In brief, the apparatus comprises a variable volume view cell, hand pump, syringe pump, and pressure indicator.

The cell's temperature was regulated using a water bath. Initially, a fixed quantity of DES and ethanol were loaded into the view cell, replacing the air with CO₂. As CO₂ was compressed into the cell, the pressure varied. Solubility, in this study, was defined as the mole fraction of DES in the system. Given the negligible amount of DES, the density of CO₂ and ethanol was computed using Aspen Plus with the Peng–Robinson equation of state, as shown in Table 3.

The pressure was adjusted until a visible phase change occurred. Under fixed composition and temperature, the bubble point pressure was established as the pressure at which the first bubbles appeared. Cloud points were also identified when the solution displayed cloudiness, indicating a phase transition from a single phase to liquid–liquid phases. To ensure consistency in the experimental results, each measurement was performed at least three times for each condition.

Experimental Data Fitting Model

In general, there are three primary approaches to calculate the solubility of solutes in scCO₂: equation of states, solubility parameter models, and empirical models. The first two methods necessitate the determination of physical parameters for DESs, which can be challenging to precisely ascertain, resulting in a lower degree of precision. Conversely, empirical models, while not reliant on the physical parameters of DESs, provide relatively reliable correlation accuracy. In this study, three models—the modified Chrastil model [24], the Kumar–Johnston model [25], and the Adachi–Lu model [26]—were employed to correlate the DES solubility data. The models varied in the number of adjustable parameters, ranging from 3 to 5. Specifically, the Kumar–Johnston model stands out with the fewest adjustable parameters at 3. However, it overlooks the influence of cosolvent presence in

Table 3 Experimentally determined bubble point or cloud points for CO₂ (1) + ethanol (2) + DES (3)

DES	T/K	$\rho/\text{g}\cdot\text{cm}^{-3,\text{a}}$	x_1	x_2	x_3	P/MPa	Phase behavior ^b
E6A1	308.2	0.573	0.597	0.363	0.040	7.24	B
E6A1	313.2	0.683	0.597	0.363	0.040	8.01	B
E6A1	318.2	0.772	0.597	0.363	0.040	8.84	B
E6A1	308.2	0.560	0.600	0.370	0.030	7.22	B
E6A1	313.2	0.675	0.600	0.370	0.030	7.89	B
E6A1	318.2	0.700	0.600	0.370	0.030	8.54	B
E6A1	308.2	0.588	0.639	0.321	0.040	7.65	C
E6A1	313.2	0.795	0.639	0.321	0.040	8.95	C
E6A1	318.2	0.789	0.639	0.321	0.040	10.06	C
E6A1	308.2	0.840	0.660	0.300	0.040	10.73	C
E6A1	313.2	0.828	0.660	0.300	0.040	12.40	C
E6A1	318.2	0.817	0.660	0.300	0.040	14.16	C
E6A1	308.2	0.849	0.680	0.280	0.040	13.69	C
E6A1	313.2	0.835	0.680	0.280	0.040	14.90	C
E6A1	318.2	0.821	0.680	0.280	0.040	16.21	C
E8A1	308.2	0.465	0.566	0.394	0.040	6.82	B
E8A1	313.2	0.528	0.566	0.394	0.040	7.48	B
E8A1	318.2	0.615	0.566	0.394	0.040	8.26	B
E8A1	308.2	0.555	0.606	0.355	0.039	7.26	B
E8A1	313.2	0.633	0.606	0.355	0.039	7.94	B
E8A1	318.2	0.756	0.606	0.355	0.039	8.80	B
E8A1	308.2	0.518	0.640	0.320	0.040	7.41	B
E8A1	313.2	0.705	0.640	0.320	0.040	8.47	B
E8A1	318.2	0.778	0.640	0.320	0.040	9.54	B
E8A1	308.2	0.852	0.683	0.277	0.040	15.72	C
E8A1	313.2	0.839	0.683	0.277	0.040	17.24	C
E8A1	318.2	0.826	0.683	0.277	0.040	18.89	C

Standard uncertainties u are $u(x_i)=0.005$; $u(T)=0.1$ K, and $u(P)=0.135$ MPa

T: temperature; x_i : mole fraction of each chemical, P: pressure

^aCalculated using Aspenplus package with the Peng–Robinson equation of state

^bB: bubble point; C: cloud point

Table 4 Regression parameters of the four-parameter Chrastil equation

DES	k	r	a	b	AARD(%)	R ²
E6A1	0.2215	0.3585	0.9997	0.8834	3.80	0.997
E8A1	1.0103	-0.0088	3.0482	-2.4667	0.25	0.997

k, r, a, and b are model parameters; AARD is the average absolute relative deviations; and R² is the correlation coefficient

Table 5 Correlation of solubility using the Kumar–Johnston three-parameter

DES	c ₀	c ₁	c ₂	AARD(%)	R ²
E6A1	2.2162	1.0060	2.5891	2.02	0.998
E8A1	2.0981	1.2891	2.6338	1.07	0.995

c₀, c₁, and c₂ are model parameters; AARD is the average absolute relative deviations; and R² is the correlation coefficient

the system, focusing solely on exploring the impact of solvent density and system temperature. In contrast, the modified Chrastil model takes into account the effects of solvent density, cosolvent content, and temperature on the solubility of DES with 4 parameters. Meanwhile, the Adachi–Lu model addresses the first two effects only but employs 5 parameters.

A semi-empirical model, originally proposed by Chrastil [23] to depict the relationship between solute solubility and the density of the supercritical fluid, was further refined by Gonzalez et al. [24]. This modification involves the assumption that solute molecule form complex molecule, as shown in Eq. (2)

$$\ln y = k \ln \rho + r \ln m + \frac{a}{T} + b \quad (2)$$

, where y (g·lit⁻¹) is the solubility of DESs, ρ (g·lit⁻¹) is density of scCO₂, and m (g·lit⁻¹) is the concentration of the ethanol. The constant k signifies an average association number for a specific solute and supercritical solvent, while r designates an average association number for the cosolvent. a is a constant linked to the enthalpies of vaporization and solvation of the solute, and b denotes model parameter. The obtained results are presented in Table 4.

Kumar and Johnston [25] introduced an empirical model wherein the density of solvent in supercritical state is

correlated with the mole fraction of the solute. The expression of the model is shown in Eq. (3)

$$\ln y = c_0 \rho + \frac{c_1}{T} + c_2 \quad (3)$$

y (g·lit⁻¹) is the solubility of DESs in solvent, ρ (g·lit⁻¹) is density of solvent of scCO₂. c₀, c₁, and c₂ are model parameters. The results are shown in Table 5.

In general, alternations in density did not exhibit a linear correspondence to changes in pressure. To account for this nonlinearity in density concerning pressure variations, the Adachi–Lu model [26] was also subjected to correlation. Taking into account the presence of a cosolvent, the Adachi–Lu model is expressed in Eq. (4).

$$\ln y = (e_0 + e_1 \rho + e_2 \rho^2) \ln \rho + e_3 y^* + e_4 \quad (4)$$

, where y (g·lit⁻¹) is the solubility of DESs, ρ (g·lit⁻¹) is density of solvent of supercritical CO₂, y* (g·lit⁻¹): mass concentration of the cosolvent of ethanol. e₀, e₁, e₂, e₃, and e₄ are model parameters. The results are shown in Table 6.

The effectiveness of the models was assessed using the average absolute relative deviation (AARD (%)), as indicated in Eq. (5).

$$\text{AARD}(\%) = \frac{100}{N - Z} \sum \left| \frac{y_i^{\text{cal}} - y_i^{\text{exp}}}{y_i^{\text{exp}}} \right| \quad (5)$$

, where y_i^{cal} represents the calculated value of the DES solubility, y_i^{exp} signifies the experimentally measured value, N denotes the number of data points, and Z represents the correlation parameters following the suggestion of Garlapati and Madras [31]. This metric represents the average deviation between experimentally determined DES solubility and that calculated by the correlation model. The parameters of the models were optimized through non-linear regression.

Table 6 Correlation of solubility using the Adachi–Lu equation

DES	e ₀	e ₁	e ₂	e ₃	e ₄	AARD(%)	R ²
E6A1	0.8722	0.0066	-1.2799	-0.3888	4.6050	4.98	0.999
E8A1	1.0508	-0.2163	0.2045	-0.0857	4.4983	0.31	0.997

e₀, e₁, e₂, e₃, and e₄ are model parameters; AARD is the average absolute relative deviations; and R² is the correlation coefficient

Results and Discussion

The bubble point and cloud point pressures for mixtures of CO₂ + ethanol + DES with varying compositions were experimentally determined over a temperature range spanning from 308.2 K to 318.2 K with a 5 K interval. The experimental data for two distinct ternary systems, namely CO₂ + ethanol + E6A1 and CO₂ + ethanol + E8A1, are presented in Table 3. In the CO₂ + ethanol + E6A1 ternary system, both bubble point pressures and cloud point pressures were observed. Specifically, when the ratios between cosolvent (ethanol) and solvent (CO₂) exceeded 0.6, bubble points were observed, and when these ratios were less than 0.5, cloud points were observed. Similar phase change patterns were observed for the CO₂ + ethanol + E8A1 system. However, when the ratios of cosolvent to solvent exceeded 0.5, bubble points were observed. Significantly, no phase transition pressures have been observed at these temperatures in the absence of ethanol, a cosolvent, up to 30 MPa, the experimental apparatus operating limit.

Effect of temperature on solubility

Both the bubble point and cloud point pressures increased with increasing the system temperature at a fixed DES mole fraction. This suggests that the solubility of DES in CO₂ and ethanol mixture decreased at higher temperature corresponding to exothermic processes [32]. When the mole fraction of E6A1 increased isothermally, the bubble point pressure correspondingly increased slightly. For example, while the bubble point pressure of 8.01 MPa was observed for 0.040 mol fraction of E6A1, that of 7.89 MPa for 0.030 at 313.2 K. To dissolve the same amount of DESs in CO₂ and ethanol mixture lower system temperature seems to be better condition. Typically, with a rise in temperature, the saturation vapor pressure of solute increases, promoting an increase in solubility [33]. However, the density of scCO₂ decreases as temperatures rise, leading to a reduction in the solubility of DES. The impact of temperature is contingent on the combined effects of these two opposing factors.

As far as cloud point pressures are concerned, similar results were also observed. For instance, the cloud point pressure of 13.69 MPa at 308.2 K increased 16.21 MPa at 318.2 K at 0.040 mol fraction of E6A1. Not only the bubble point but also the cloud point pressures for E8A1 were also followed similar trends, as shown in Fig. 1.

Effect of Ratio of Cosolvent to Solvent on Solubility

As the mole ratio between ethanol and CO₂ decreased, the cloud point pressure correspondingly increased significantly.

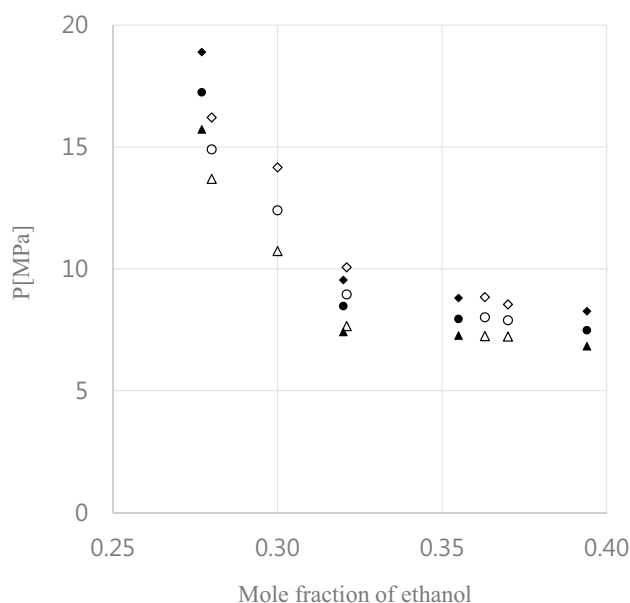


Fig. 1 P-x diagram of CO₂ (1)+ethanol (2)+DES (3) system at different temperatures. (open triangle: 308.2 K-E6A1; filled triangle: 308.2 K-E8A1; open circle: 313.2 K-E6A1; filled circle: 313.2 K-E8A1; open diamond: 318.2 K-E6A1; filled diamond: 318.2 K-E8A1)

For instance, at 308.2 K while the mole ratio was 0.502, the cloud point pressure was 7.65 MPa, and when the mole ratio was 0.412, it was 13.69 MPa at 308.2 K for E6A1. In case of E8A1, similar results were observed. Specifically, when the mole ratio was 0.696, the bubble point pressure was 8.26 MPa, and when the mole ratio was 0.500, it was 9.54 MPa at 318.2 K.

As the amount of cosolvent ethanol increased, the bubble point or cloud point pressure decreased significantly. This means that the solvation power of CO₂ is considerably low that the addition of ethanol raises the solvation power significantly. CO₂'s solvent power is not strong enough to dissolve CO₂-philic compounds, as Beckman reported [1]. So, it would be such a meaningful approach to add ethanol as a cosolvent to enhance the solubility of DESs.

Effect of Pressure on Solubility

In general, with an increase in pressure at constant temperature, the solubility of DESs demonstrated a corresponding increase. For instance, the solubility of E6A1 was 0.030 at 8.54 MPa, and it increased to 0.040 at 8.84 MPa at 318.2 K. The pressure effect can be attributed to the rising values of the variable leading to an increase in fluid density, consequently enhancing the solvent power of scCO₂. The solvent densities at 8.54 MPa and 318.2 K, and 8.84 MPa and 318.2 K were 0.7002 and 0.7723 g·cm⁻³, respectively. However, the impact of density alone is not sufficient to elucidate

the increase in DES solubility. A plausible explanation for this nonlinear dependence on solvent density on DES solubility could be that the density of scCO_2 and the ethanol solvent converges toward the liquid phase with increasing pressure. However, as the compressibility of scCO_2 diminishes when it approaches the liquid phase, the density of scCO_2 and the ethanol solvent experiences a slight increase rising pressure in higher pressure ranges, as shown in Table 3.

Data Correlation

In this study, the experimental data were correlated with three models: the modified Chrastil equation, the Kumar–Johnston equation, and the Adachi–Lu equation, as briefly outlined in Sect. "Experimental data fitting model". Tables 4, 5, 6 present the correlation parameters and AARDs between the experimental and calculated solubility of two DESs. The result from the modified Chrastil model indicated AARD of 3.80% for $\text{CO}_2 + \text{ethanol} + \text{E6A1}$ and 0.25% for $\text{CO}_2 + \text{ethanol} + \text{E8A1}$. Notably, for $\text{CO}_2 + \text{ethanol} + \text{E8A1}$, the modified Chrastil model demonstrated the lowest AARD values at 0.25%. In the case of $\text{CO}_2 + \text{ethanol} + \text{E8A1}$, the Kumar–Johnston model exhibited the lowest AARD values at 2.02%. Despite having five parameters, the Adachi–Lu model demonstrated higher AARD values for both the $\text{CO}_2 + \text{ethanol} + \text{E6A1}$ and $\text{CO}_2 + \text{ethanol} + \text{E8A1}$ systems. As anticipated, the modified Chrastil model exhibited lower deviation in the case of $\text{CO}_2 + \text{ethanol} + \text{E8A1}$ due to its consideration of solvent density, cosolvent content, and temperature effects on the solubility of DES. In the case of $\text{CO}_2 + \text{ethanol} + \text{E6A1}$, the Adachi–Lu model yielded the lowest AARD values, indicating that solvent density and temperature effects may be predominant in E6A1 DES solubility. Nevertheless, all three models exhibited a high degree of fitting to the experimental data, with R^2 values approaching unity and AARD values converging toward zero percent.

Conclusions

The high-pressure phase behavior of $\{\text{CO}_2 + \text{ethanol} + \text{E6A1}\}$ was investigated using a high-pressure variable-volume view cell, covering temperatures from 308.2 K to 318.2 K and pressures up to 18.89 MPa. At a constant temperature, the solubility of the DES in $\text{scCO}_2 + \text{ethanol}$ increased with pressure. Besides the bubble point pressure, cloud point pressures were observed when the mole ratios of ethanol to scCO_2 were below 0.502. The phase behavior of $\{\text{CO}_2 + \text{ethanol} + \text{E8A1}\}$ was also examined to explore the impact of the mole ratio between ethylene glycol as a hydrogen bond donor and allyltriphenylphosphonium bromide as a hydrogen bond acceptor. Similar to the $\{\text{CO}_2 + \text{ethanol} + \text{E6A1}\}$ ternary system, the $\{\text{CO}_2 + \text{ethanol} + \text{E8A1}\}$

ternary system exhibited both bubble point and cloud point pressures at high pressure. Generally, as the mole ratio between HBD and HBA increased from 6:1 to 8:1, both bubble point and cloud point pressures also increased. This outcome could be attributed to the heightened interaction between ethylene glycol (HBD) and ethanol (cosolvent) at the molecular level. The solubility of DESs in $\text{scCO}_2/\text{ethanol}$ mixture increased with rising pressure, possibly due to the enhanced solvent power of scCO_2 . The experimental data were effectively correlated with three models—the modified Chrastil equation, the Kumar–Johnston equation, and the Adachi–Lu equation—with average absolute relative deviations falling in the range of 0.25–4.98%.

Acknowledgements This research was supported by Basic Science Research Program through the National Research Foundation of Korea (NRF) funded by the Ministry of Education, Science and Technology (NRF-2020R1F1A10488128). This work was supported by 2023 Hongik University Research Fund.

Data availability All data supporting the findings of this study are available within the paper.

References

1. E. Beckman, *Chem. Comm.*, 1885 (2004).
2. P. Raveendran, S.L. Wallen, *J. Am. Chem. Soc.* **124**, 12590 (2002)
3. Y. Park, R.B. Gupta, C.C. Curtis, C.B. Roberts, *J. Phys. Chem. B* **106**, 9696 (2002)
4. P.W. Bell, A.J. Thote, Y. Park, R.B. Gupta, C.B. Roberts, *Ind. Eng. Chem. Res.* **42**, 6280 (2003)
5. M.S. Manic, A.J. Queimada, E.A. Macedo, V. Najdanovic-Visak, *J. Supercrit. Fluid* **65**, 1 (2012)
6. Y. Park, *J. Supercrit. Fluids* **36**, 154 (2005)
7. J. Wang, Z. Song, L. Chen, T. Xu, L. Deng, Z. Qi, *Green. Chem. Eng.* **2**, 431–440 (2021)
8. P.A. Mercadal, M.L. Picchio, A. Gonzalez, *Food Hydrocolloids* **147**, 109414 (2024)
9. R. Al-Frasi, M. Hayyan, *Renew. Sust. Energy. Rev.* **184**, 113505 (2023)
10. A.K. Lavrinenko, I.Y. Chernyshov, E.A. Pidko, *ACS Sustainable Chem. Eng.* **11**, 15492 (2023)
11. Y. Park, *Korean J. Chem. Eng.* **38**, 604 (2021)
12. M. Jung, Y. Park, *J. Chem. Eng. Data* **67**, 416 (2022)
13. Y. Park, J. Lee, *J. Solution Chem.* **52**, 413 (2023)
14. S.N.V.K. Aki, A.M. Scurto, J.F. Brennecke, *Ind. Eng. Chem. Res.* **45**, 5574 (2006)
15. W. Wu, W. Li, B. Han, T. Jiang, D. Shen, Z. Zhang, D. Sun, B. Wang, *J. Chem. Eng. Data* **49**, 1597 (2004)
16. G. Li, D. Zhou, Q.Q. Xu, G.Y. Qiao, J.Z. Yin, *J. Chem. Eng. Data* **63**, 1596 (2018)
17. Z. Zhang, W. Wu, Z. Liu, B. Han, H. Gao, T. Jiang, *Phys. Chem. Chem. Phys.* **6**, 2352 (2004)
18. M.B. Haider, P. Maheshwari, R. Kumar, *J. Env. Chem. Eng.* **9**, 106727 (2021)
19. S. Sarmad, Y. Xie, J.P. Mikkola, X. Ji, *New J. Chem.* **41**, 290 (2017)
20. X. Liu, B. Gao, Y. Jiang, D. Deng, *J. Chem. Eng. Data* **62**, 1448 (2017)
21. M.S. Alhajeri, Z. Wu, D. Rincon, F. Albalawi, P.D. Christofides, *Chem. Eng. Res. Des.* **167**, 268 (2021)

22. S. Malik, V.K. Sharma, *Korean J. Chem. Eng.* **40**, 2581 (2023)
23. J. Chrastil, *J. Phys. Chem.* **86**, 3016 (1982)
24. J.C. González, M.R. Vieytes, A.M. Botana, J.M. Vieites, K.M. Botana, *J. Chromatogr. A* **910**, 119 (2001).
25. S.K. Kumar, K.P. Johnston, *J. Supercrit. Fluids* **1**, 15 (1988)
26. Y. Adachi, B.C.-Y. Lu, *Fluid Phase Equilib.* **1983**(14), 147 (1983)
27. Y. Ozbakir, C. Erkey, *J. Supercrit. Fluids* **98**, 153 (2015)
28. S.Y. Hwang, Y. Park, K. Park, *J. Chem. Thermodyn.* **43**, 339 (2011)
29. S.Y. Hwang, Y. Park, K. Park, *J. Chem. Eng. Data* **57**, 2160 (2012)
30. M. Kim, J. Lee, S. Lee, Y. Park, *J. Chem. Thermodyn.* **121**, 91 (2018)
31. C. Garlapati, G. Madras, *Thermochim. Acta* **500**, 123 (2010)
32. F.P. Pelaquim, A.M.B. Neto, I.A.L. Dalmolin, M.C. da Costa, *Ind. Eng. Chem. Res.* **60**, 8607 (2021)
33. X. Zha, S. Han, W. Wang, Z. Jiao, *J. Chem. Thermodyn.* **131**, 104 (2019)

Publisher's Note Springer Nature remains neutral with regard to jurisdictional claims in published maps and institutional affiliations.

Springer Nature or its licensor (e.g. a society or other partner) holds exclusive rights to this article under a publishing agreement with the author(s) or other rightsholder(s); author self-archiving of the accepted manuscript version of this article is solely governed by the terms of such publishing agreement and applicable law.